OPEN

Highly Electrically Conductive Nanocomposites Based on Polymer-Infused Graphene Sponges

Yuanqing Li[1], Yarjan Abdul Samad[1], Kyriaki Polychronopoulou[2], Saeed M. Alhassan[3] & Kin Liao[1]

[1]Department of Aerospace Engineering, Khalifa University of Science, Technology, & Research, Abu Dhabi 127788, UAE, [2]Department of Mechanical Engineering, Khalifa University of Science, Technology, & Research, Abu Dhabi 127788, UAE, [3]Department of Chemical Engineering, The Petroleum Institute, Abu Dhabi 2533, UAE.

Conductive polymer composites require a three-dimensional (3D) network to impart electrical conductivity. A general method that is applicable to most polymers for achieving a desirable graphene 3D network is still a challenge. We have developed a facile technique to fabricate highly electrical conductive composite using vacuum-assisted infusion of epoxy into graphene sponge (GS) scaffold. Macroscopic GSs were synthesized from graphene oxide solution by a hydrothermal method combined with freeze drying. The GS/epoxy composites prepared display consistent isotropic electrical conductivity around 1 S/m, and it is found to be close to that of the pristine GS. Compared with neat epoxy, GS/epoxy has a 12-orders-of-magnitude increase in electrical conductivity, attributed to the compactly interconnected graphene network constructed in the polymer matrix. This method can be extended to other materials to fabricate highly conductive composites for practical applications such as electronic devices, sensors, actuators, and electromagnetic shielding.

Graphene, a two-dimensional mono-layer of carbon atoms, has attracted much attention due to its fascinating properties such as high electrical conductivity, high thermal conductivity, extraordinary elasticity, and stiffness etc[1–5]. It has been shown that adding graphene to polymers can enhance the mechanical, electrical, and thermal properties of the resulting nanocomposites[6–10]. Graphene-based polymer composites with high electrical and thermal conductivity are highly desirable in many practical applications such as electronic device, electromagnetic shielding, and thermal management[10–14].

However, there are two factors limiting the application of graphene-based polymer composites: (1) poor dispersion of graphene in a polymeric matrix due to their high specific surface area and strong intermolecular interactions between graphene sheets; which limits the improvements of material properties in polymer composites, (2) at low filler content, graphene sheets are covered by polymer chains; which doesn't allow the sheets to reach a percolation limit in the mixture. Since the electrical and thermal conductivity of these composites strongly rely on electron and phonon percolation between the separated filler particles[14–16], a good dispersion of graphene sheets and high filler content are required to form a conductive interconnected network in the insulating polymer matrix to improve the conductivity of the composites[17].

To improve the dispersion of graphene in a polymer matrix, a great deal of efforts has been made using the strategy of molecular functionalization. Nonetheless, those functional groups, while improving dispersion, damage the electronic conjugation of graphene sheets, thus, compromising the conductivity of the composite. Despite the improved homogeneous distribution, however, the electrical conductivity of these composites is still far below the expected level, due to high inter-sheet junction contact resistance amongst graphene sheets, arising from the functional groups between graphene sheets and the polymer matrix[16]. Furthermore, a high loading of fillers generally hampers the process ability and overall properties of the composites due to severe agglomeration and poor interfacial bonding[14,18].

Conductive polymer composites require a three-dimensional (3D) network to impart electrical conductivity. The construction of a 3D, compactly interconnected graphene network can offer a significant increase in electrical and thermal conductivity of polymer composites. *Wu et al.*, have developed a self-assembly and hot press technique for fabricating polystyrene composites with 3D interconnected graphene networks[16]. *Chen et al.* reported a highly conductive poly(dimethyl siloxane) composite films with 3D graphene foam using a template-directed chemical vapor deposition method[14]. The compact contact between graphene sheets in the 3D

architecture and high reduction level of graphene sheets render remarkable electrical conductivity to the composites. However, these methods are complicated and can only be used to fabricate specific polymer (thermoplastic) or composite foam; a general method that is applicable to most polymers for achieving a desirable graphene 3D network is still a challenge.

Recently, assembling graphene sheets into 3D graphene sponge (GS) was realized by hydrothermal treatment combined with freeze drying technology[19–21]. This process to fabricate GS is facile, low-cost, and scalable, and it opens an innovative field of fabricating highly conductive graphene composites. Here we demonstrate the fabrication of a highly conductive GS/epoxy composite with GS as scaffold infiltrated with epoxy resin. The composite samples were fabricated by a simple vacuum assisted infusion process, in which the GS was prepared by hydrothermal method combined with freeze drying. Results show that the 3D network of GS remains intact after the infusion process, and electrical conductivity of the GS/epoxy composites is comparable with the GS. Moreover, by filling the GS with other selected materials, highly conductive composites can be made for practical applications such as electronic devices, sensors, actuators, and electromagnetic shielding.

Results

Macroscopic graphene sponges were synthesized from GO solution by a hydrothermal method combined with freeze drying, as shown schematically in Fig. 1. GO is hydrophilic and can be well dispersed into water to form a stable suspension. With hydrothermal treatment, GO was reduced by HI to form hydrophobic graphene. The increased hydrophobicity, van der Waals forces, and π-π stacking interactions of graphene sheets lead to aggregation. After high temperature and high pressure treatment, much water was expelled from the aggregates and a 3D network of compacted graphene sheets was formed. The as-prepared 3D graphene is a hydrogel with plenty of water remaining inside. Finally, a black 3D graphene sponge, as shown in Fig. 2 (a), is obtained by freeze drying the as-prepared graphene hydrogel.

The GS obtained is ultra-light with a density of 0.022 g/cm³. The internal morphology of the GS was observed using SEM. Typical low- and high-magnification SEM images of GS are shown in Figs. 2 (b) and (c). It is shown from the SEM images that the GS has a 3D porous structure, with pore size in the range of a few to several microns. Interconnected porous with many wrinkles can be seen in the high-magnification SEM image, indicating the formation of 3D network structure *via* aggregation of reduced GO sheets. The electrical conductivity of GS measured is 0.217 S/m. In addition, the electrical conductivity of GSs is isotropic, attributed to the randomly aggregated reduced GO sheets.

The pore size, density, and properties of GSs can be tuned by pre-drying the graphene hydrogel before freeze drying. It was found that the pre-drying process did not change the shape of graphene hydrogel, pre-drying only resulted in the shrinkage of the sample dimensions and an increase in density. The density of GS-50 and GS-75 is 0.041 and 0.086 g/cm³ respectively (compared with GS's 0.022 g/cm³). A cross-sectional image of GS-75 is shown in Fig. 2(d), it is clear that with increasing density, the stack of graphene sheets become compact and the pore size of GS decreases to the range of several hundred nanometers to around 2 microns. The porosimetry measurements show that the specific surface area of GS, GS-50, and GS-75 is 4.97, 10.99, and 30.44 m²/cm³, respectively. From the pore volume distribution curve (Fig. 3 (a)), it is clear that GS-75 and GS-50 presents higher population of mesoporosity and microporosity than the original GS, which leads to the increase of specific surface area. The increased mesoporosity of GS-75 and GS-50 is also supported by the shape of the hysteresis loop (Figure S1). Furthermore, GS-75 presents a higher N_2 adsorption at low pressures, indicating more micropores than GS-50 and GS. At the same time, with an increase in GS density, the interconnection between the graphene sheets is enhanced, which leads to the enhancement of electrical conductivity - the electrical conductivities of GS-50 and GS-75 are 0.509 and 2.32 S/m, respectively (Fig. 3(b)).

As prepared graphene sponges have an open pore structure, thus polymers, such as epoxy resin, can be infused into the sponge. As illustrated in Fig. 1, the graphene sponge is used as a scaffold to infuse with epoxy resin, and the open pores are completely filled. To facilitate the infusion of viscous fluid, GS/epoxy mixture were placed in a vacuum chamber for approximately 10 min. When completely cured, the composite maintains the same original shape and overall size (Fig. 3(b) inset), indicating that little deformation or shrinkage occurs during the infusion process. The electrical conductivity of GS/epoxy composites at different GS content is also shown in Fig. 3(b). Pure epoxy resin without GS is almost an insulator with a conductivity of around 10^{-13} S/m. The electrical conductivity of GS/epoxy,
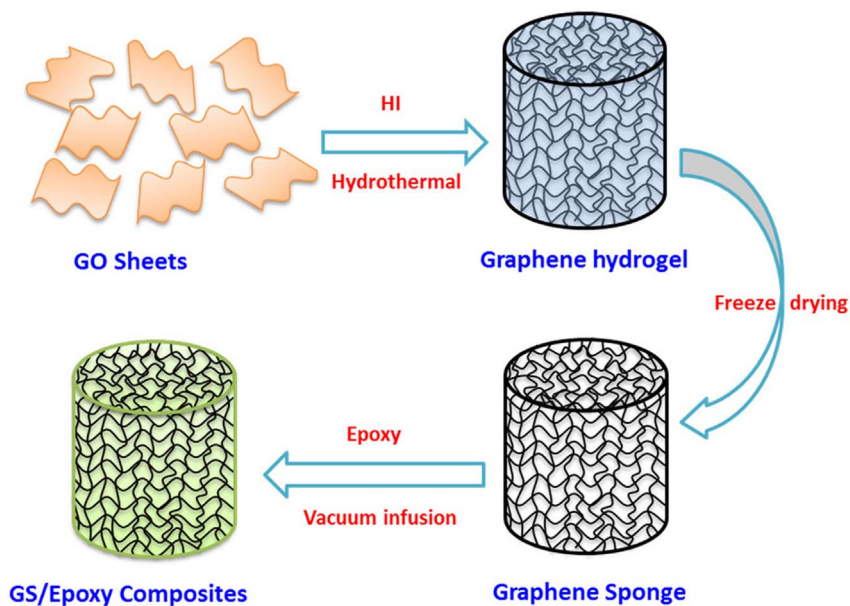

Figure 1 | Schematics of the fabrication processes of GS/epoxy nanocomposite.
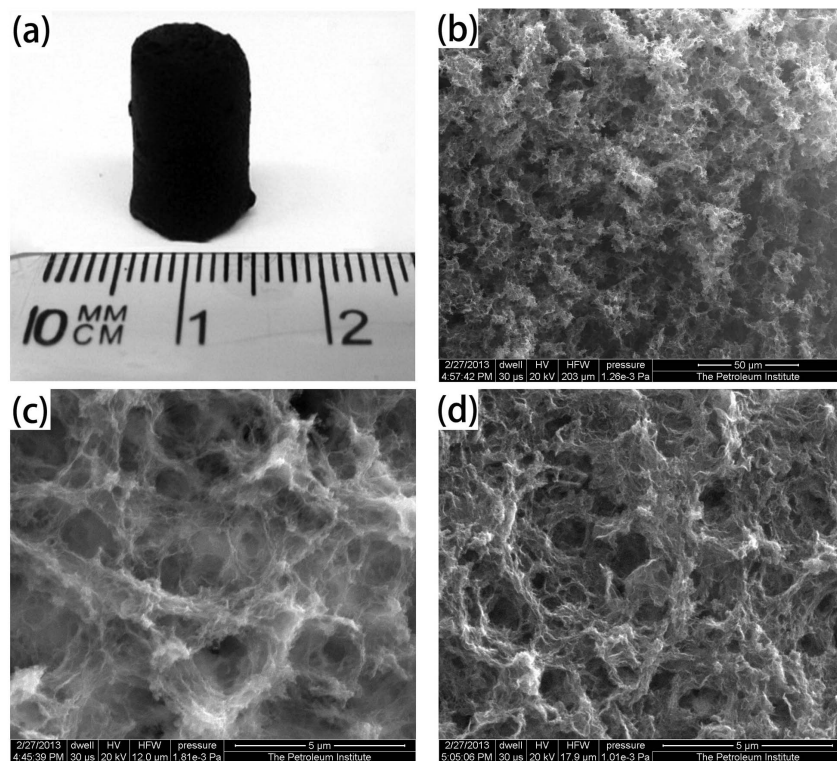
Figure 2 | Image of a GS sample (a), SEM images of inner structure of GS (b) and (c), and GS-75 (d).

GS-50/epoxy, and GS-75/epoxy is 0.21, 0.41, and 1.73 S/m, respectively. In addition, the electrical conductivities along three perpendicular directions of the sample were also measured and the results are very close. The isotropic electrical property of the composites is attributed to the random arrangement of graphene sheets in the GS. Compared with pure epoxy, a 12-order-of-magnitudes increase in the electrical conductivities of GS/epoxy is seen. Remarkably, the electrical conductivity of GS/epoxy is very close to that of the pristine GS. Although GS-75/epoxy suffers highest drop in electrical conductivity, it was only 30% less than that of the pristine GS-75, which is still a remarkable improvement compared with that of pure epoxy. Based on our knowledge, the electrical conductivity of GS/epoxy produced in this work is at least one order of magnitude higher than the best electrical conductivity of graphene/epoxy composites (with similar filler content) ever reported (Table 1). For the graphene/epoxy composites prepared with traditional methods[22–27], it is difficult to obtain interconnected graphene network and achieve the electron percolation at low filler content due to the hindering of polymer chain. The good electrical conductivity of GS/epoxy reported in this work attribute to the compactly interconnected graphene network constructed in the polymer matrix as proved at discussion section. Furthermore, it should be noted that the electrical conductivity of GS/epoxy is directly related to that of the GS, which can be further improved *via* post-treatment of GS.

The cross-sectional SEM images of GS/epoxy nanocomposites are shown in Fig. 4. It can be seen that the porous space in the pristine sponge is almost entirely filled up with epoxy resin. In addition, the GS/epoxy nanocomposites show a rough fracture surface with some irregular protuberances, owing to the embedding of graphene sponge in the epoxy matrix. Furthermore, it is clear that the fracture surface of GS-75/epoxy exhibits a higher roughness than GS/epoxy, due to high filler content. In order to further investigate the effect of infusion of epoxy into the network structure of GS, epoxy matrix was washed away by acetone before it was completely cured. After washing, the GS maintains the same original shape and overall size with no visible damage, indicating that infusion of epoxy was carried out

smoothly without disturbing the intrinsic structure and morphology of the sponge, and conduction pathways of the graphene networks are preserved.

Discussion

The GS/epoxy nanocomposites fabricated have comparable electrical conductivity with pristine GS. From above discussion, it seems that the most important factor for high electrical conductivity should be a 3D compactly interconnected graphene network constructed in the polymer matrix. To further prove the significance of preserving 3D network structure for the electrical conductivity, pre-crushed GS/epoxy (PC-GS/epoxy) composite samples were prepared by manually compressing the GS/epoxy, before completely curing of the composites. Compared with GS/epoxy, as shown in Fig. 3(b), the electrical conductivity of the PC-GS/epoxy samples is at least 5 orders of magnitudes less. As shown in Fig. 5(a), many white-colored wavy ridges and fragments are seen on the fracture surface of PC-GS/epoxy. The white color of these parts reveals the low electrical conductivity of corresponding materials, indicating that the interconnected graphene network was destroyed, cracks are generated and filled with insulation epoxy by compression. After washing away the epoxy matrix, the 3D GS structure was broken into small pieces, which further proves the damage of 3D structure of GS. Therefore, the preserved interconnected graphene network is critical to achieve high electrical conductivity. As shown schematically in Fig. 5 (b), cracks from graphene network can be generated by compression and will be filled by insulation epoxy resin, which lead to the disruption of graphene network and significant drop in the electrical conductivity.

In summary, macroscopic graphene sponges were synthesized from GO solution by a hydrothermal method combined with freeze drying. The pore size, density, and properties of GSs can be tuned by pre-drying the graphene hydrogel. Highly electrically conductive GS/epoxy composites were fabricated by vacuum assisted infusion of epoxy into the GS scaffold. The GS/epoxy composites display isotropic electrical behavior, with improved and consistent conductivity measured along any direction. Compared with neat epoxy, the
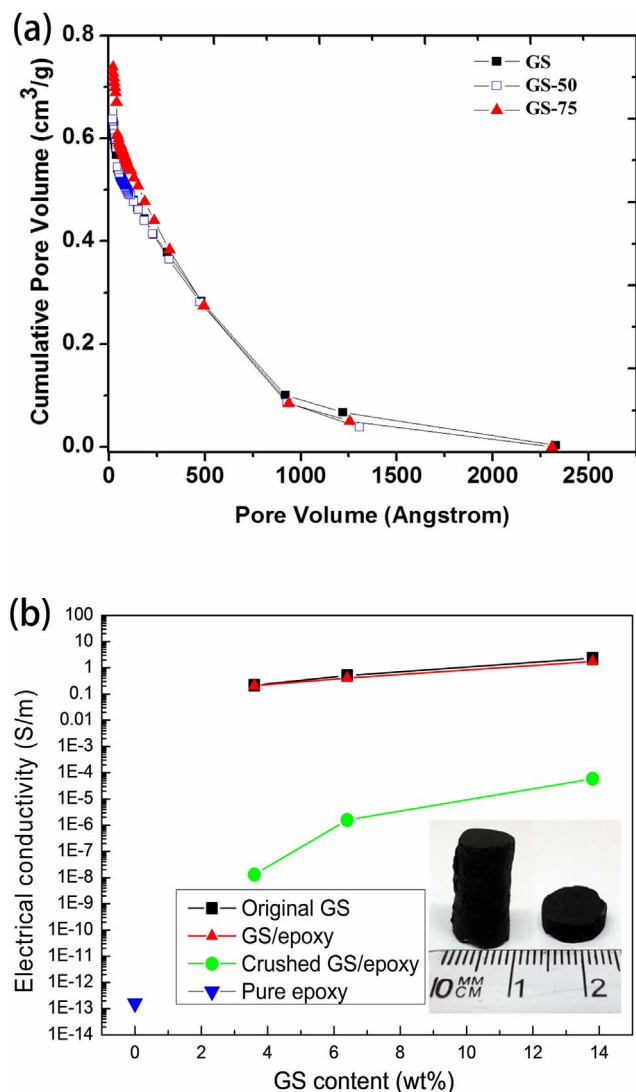
Figure 3 | (a) The cumulative pore volume of GS, GS-50 and GS-75. (b) Electrical conductivity of pure epoxy, GS, GS/epoxy, and PC-GS/epoxy; and optical images of GS/epoxy composites with different sizes (inset).

electrical conductivity of GS/epoxy has increased around 12 orders of magnitudes. In addition, the electrical conductivity of GS/epoxy is very close to that of the pristine GS. The results reveal that the 3D compactly interconnected graphene network constructed in the polymer matrix is critical for high electrical conductivity. The method presented herein is versatile, by filling the excellent interconnected graphene network of GS with other selected materials, other highly electrically conductive composites can be created.

Methods

Materials. Graphite powder with particle size <20 μm, concentrated sulfuric acid (H_2SO_4, 98%), potassium persulfate ($K_2S_2O_8$), phosphorus pentoxide (P_2O_5), sodium
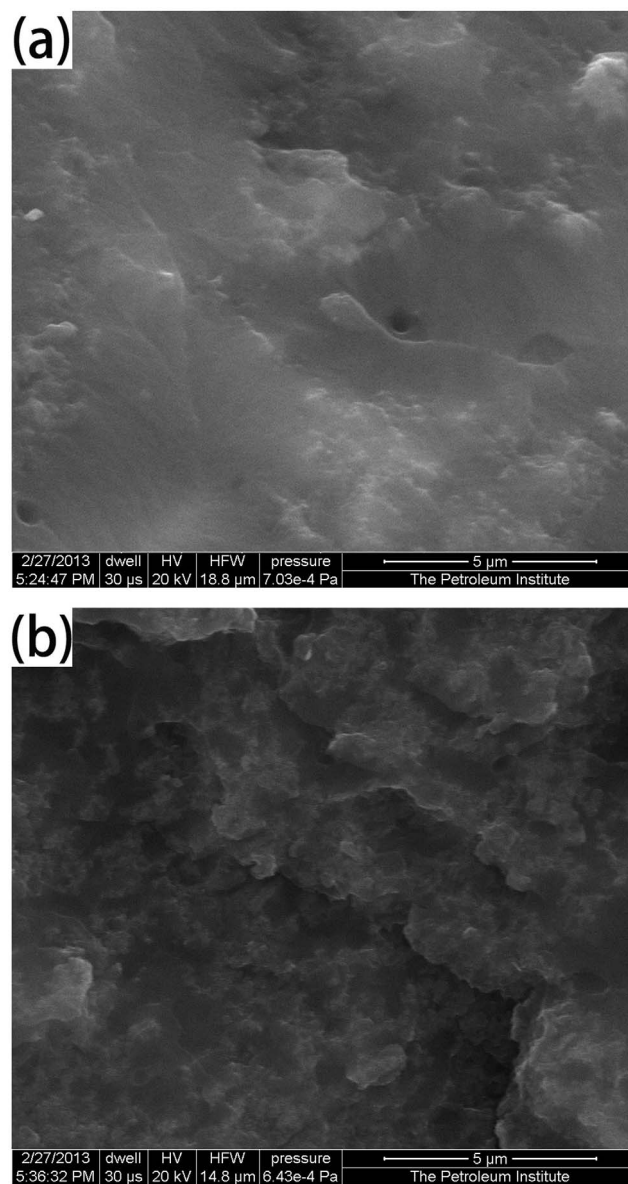
Figure 4 | SEM images of fracture surface of (a) GS/epoxy and (b) GS-75/epoxy samples.

nitrate ($NaNO_3$), hydrochloric acid (HCl), potassium permanganate ($KMnO_4$), ethanol, and hydrogen peroxide (H_2O_2, 30%), hydroiodic acid (HI, 30%) were obtained from Sigma-Aldrich Co. Ltd. 635 Thin Epoxy, a room temperature two component curing system, was obtained from US Composites Inc. All of the materials were directly used without further purification.

Preparation of GO sheets. GO was synthesized from graphite powder with modified Hummer's method[28,29]. First, $K_2S_2O_8$ (10 g) and P_2O_5 (10 g) were dissolved in concentrated H_2SO_4 (50 ml) at 80°C. Graphite powder (12 g) was then added to the acidic solution, and the resulting mixture was stirred at 80°C for 4.5 h. After cooling to room temperature, the solution was diluted with about 2 L deionized (DI) water

Table 1 | The electrical conductivity of different graphene/epoxy composites

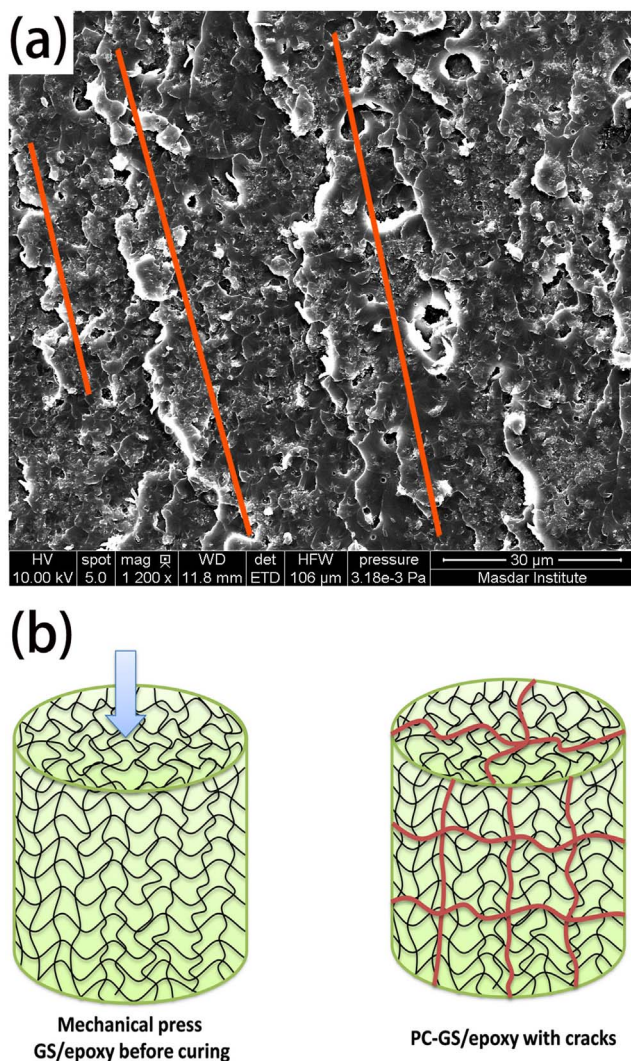| Reference	Type of Filler	Filler content	Electrical Conductivity (S/m)
Present work	Graphene sponge	~2 wt%	0.21
An et al.[22]	Graphene	2 wt%	0.01
Bao et al.[23]	Graphene oxide	2 wt%	10^{-10}
Cao et al.[24]	Graphene	2 wt%	3.28×10^{-3}
Liang et al.[25]	Graphene	2 wt%	$10^{-5.5}$
Ma et al.[26]	Graphene	0.98 vol%	8.3×10^{-7}
Monti et al.[27]	Graphene nanoplatelets	2 wt%	10^{-5}

Figure 5 | (a) SEM image of fracture surface of PC-GS/epoxy, red-colored lines indicate the direction of cracks; (b) Schematic of inner structure of GS/epoxy and PC-GS/epoxy, cracks are represented by red-colored lines.

Preparation of GS/epoxy nanocomposites. Epoxy and curing agent were mixed homogenously *via* magnetic stirring. The weight ratio of epoxy resin to curing agent was kept at 3 : 1. The GS prepared was completely immersed into the epoxy mixture. Then the mixture was placed in a vacuum chamber for approximately 10 min for the GS to be infused with epoxy and to remove air bubbles. Finally, the GS/epoxy sample was taken out from epoxy mixture and cured at room temperature for 24 h. Excessive epoxy adhered to the sponge surface was removed before curing. The graphene loading in the composite was determined by measuring the weight of the graphene sponge before infusion and of the composite after epoxy infusion.

Characterization. The morphology of GS and GS/epoxy nanocomposites were examined by a FEI Quanta FEG 250 scanning electron microscopy (SEM). Images of GS and GS/epoxy composites were taken using a Canon digital camera (IXUS 70). Porosimetry measurements were carried out using a high- resolution Micromeritics 3Flex adsorption instrument. The 3Flex (Micromeritics) was equipped with high-vacuum system, and three 0.1 Torr pressure transducers. Electrical properties of the GS and GS/epoxy composites were measured at RT with a two-probe method using an insulation resistance meter (TH 2684A (10 kΩ $\sim$ 100 TΩ)) and an ADM-930 Digital Multimeter (0.1 Ω $\sim$ 40 MΩ). The specimens used for the conductivity measurement were silver-pasted to minimize the contact resistance between the composites and the electrodes. The electrical conductivity, σ, can be calculated from the equation: $\sigma = H/R \cdot A$, where H, R, and A are thickness, resistance, and area, respectively.

and was allowed to stand overnight. The supernatant was decanted, and the pre-treated graphite was obtained by centrifugation and washed three times with DI water. The product obtained was dried in air at 100°C for 12 h. This pre-treated graphite powder (2 g) was put into concentrated H$_2$SO$_4$ (50 ml) with ice bath. KMnO$_4$ (7 g) and NaNO$_3$ (1 g) were added gradually with stirring, and the temperature of the solution was kept below 10°C. The mixture was then stirred at 35°C for 2 h and DI water (96 ml) was added. The solution was stirred for another 30 min, the reaction was then terminated by adding 300 ml of DI water and 5 ml of 30% H$_2$O$_2$ solution. The mixture was centrifuged and subjected to several cycles of suspension in 5% HCl solution and was separated by centrifugation. In order to completely remove metal ions and acids, the graphite oxide was subjected to cycles of washing with DI water and separated with centrifugation until the pH value of the supernatant reached 6. The GO product was suspended in distilled water to give a viscous, brown dispersion.

Preparation of graphene sponges. The GO suspension obtained was diluted to 2 mg/ml, and was then ultrasonicated in an ultrasonic bath for half an hour. The GSs were subsequently fabricated by hydrothermal treatment of GO suspensions with the assistance of HI[19,20]. First, 1 ml of HI (30%) was added into 60 ml homogeneous GO (2 mg/ml) aqueous solution, and then the mixture was sealed in a 100 ml Teflon-lined stainless steel autoclave and maintained at 180°C for 12 h. The reactor was allowed to cool down to room temperature (RT), and the as-prepared graphene hydrogels were taken out from reactor and dipped into distilled water for 24 h to remove the residual HI. To control the density of the final GS, water from the original graphene hydrogels were partially removed in air through evaporation at RT. Finally, the samples were freezed with liquid nitrogen and freeze-dried in vacuum to remove the remaining water to obtain GS. Three type samples with 0, 50, and 75 percent by weight (wt%) water removed from graphene hydrogel before freeze drying were prepared and named as GS, GS-50, and GS-75 respectively.

1. Balandin, A. A. *et al.* Superior thermal conductivity of single-layer graphene. *Nano Lett.* **8**, 902–907 (2008).
2. Castro Neto, A. H., Guinea, F., Peres, N. M. R., Novoselov, K. S. & Geim, A. K. The electronic properties of graphene. *Rev. Mod. Phys.* **81**, 109–162 (2009).
3. Geim, A. K. & Novoselov, K. S. The rise of graphene. *Nat. Mater.* **6**, 183–191 (2007).
4. Novoselov, K. S. *et al.* Two-dimensional gas of massless Dirac fermions in graphene. *Nature* **438**, 197–200 (2005).
5. Lee, C., Wei, X. D., Kysar, J. W. & Hone, J. Measurement of the elastic properties and intrinsic strength of monolayer graphene. *Science* **321**, 385–388 (2008).
6. Li, Y. Q., Yu, T., Yang, T. Y., Zheng, L. X. & Liao, K. Bio-Inspired Nacre-like Composite Films Based on Graphene with Superior Mechanical, Electrical, and Biocompatible Properties. *Adv. Mater.* **24**, 3426–3431 (2012).
7. Li, Y. Q., Umer, R., Samad, Y. A., Zheng, L. X. & Liao, K. The effect of the ultrasonication pre-treatment of graphene oxide (GO) on the mechanical properties of GO/polyvinyl alcohol composites. *Carbon* **55**, 321–327 (2013).
8. Li, Y. Q., Yang, T. Y., Yu, T., Zheng, L. X. & Liao, K. Synergistic effect of hybrid carbon nantube-graphene oxide as a nanofiller in enhancing the mechanical properties of PVA composites. *J. Mater. Chem.* **21**, 10844–10851 (2011).
9. Song, S. H. *et al.* Enhanced Thermal Conductivity of EpoxyGraphene Composites by Using Non-Oxidized Graphene Flakes with Non-Covalent Functionalization. *Adv. Mater.* **25**, 732–737 (2013).
10. Huang, X., Qi, X. Y., Boey, F. & Zhang, H. Graphene-based composites. *Chem. Soc. Rev.* **41**, 666–686 (2012).
11. Balandin, A. A. Thermal properties of graphene and nanostructured carbon materials. *Nat. Mater.* **10**, 569–581 (2011).
12. Thomassin, J. M., Jerome, C., Pardoen, T., Bailly, C., Huynen, I., Detrembleur, C. Polymer/carbon based composites as electromagnetic interference (EMI) shielding materials. *Mater. Sci. Eng. R-Rep.* **74**, 211–32 (2013).
13. Hong, W. J., Xu, Y. X., Lu, G. W., Li, C. & Shi, G. Q. Transparent graphene/PEDOT-PSS composite films as counter electrodes of dye-sensitized solar cells. *Electrochem. Commun.* **10**, 1555–1558 (2008).
14. Chen, Z. P., Xu, C., Ma, C. Q., Ren, W. C. & Cheng, H. M. Lightweight and Flexible Graphene Foam Composites for High-Performance Electromagnetic Interference Shielding. *Adv. Mater.* **25**, 1296–1300 (2013).
15. Vuluga, D. *et al.* Straightforward synthesis of conductive graphene/polymer nanocomposites from graphite oxide. *Chem. Comm.* **47**, 2544–2546 (2011).
16. Wu, C. *et al.* Highly Conductive Nanocomposites with Three-Dimensional, Compactly Interconnected Graphene Networks via a Self-Assembly Process. *Adv. Funct. Mater.* **23**, 506–513 (2013).
17. Zhong, Y. J., Zhou, M., Huang, F. Q., Lin, T. Q. & Wan, D. Y. Effect of graphene aerogel on thermal behavior of phase change materials for thermal management. *Sol. Energ. Mat. Sol. Cells* **113**, 195–200 (2013).
18. Li, Y. Q. *et al.* Synergistic toughening of epoxy with carbon nanotubes and graphene oxide for improved long-term performance. *Rsc Adv.* **3**, 8849–8856 (2013).
19. Bi, H. C. *et al.* Spongy Graphene as a Highly Efficient and Recyclable Sorbent for Oils and Organic Solvents. *Adv. Funct. Mater.* **22**, 4421–4425 (2012).
20. Zhao, J. P., Ren, W. C. & Cheng, H. M. Graphene sponge for efficient and repeatable adsorption and desorption of water contaminations. *J. Mater. Chem.* **22**, 20197–20202 (2012).
21. Chen, W. F. & Yan, L. F. In situ self-assembly of mild chemical reduction graphene for three-dimensional architectures. *Nanoscale* **3**, 3132–3137 (2011).
22. An, J. E. & Jeong, Y. G. Structure and electric heating performance of graphene/epoxy composite films. *Eur. Polym. J.* **49**, 1322–1330 (2013).

23. Bao, C. L. *et al.* In situ preparation of functionalized graphene oxide/epoxy nanocomposites with effective reinforcements. *J. Mater. Chem.* **21**, 13290–13298 (2011).
24. Cao, L. J. *et al.* How a bio-based epoxy monomer enhanced the properties of diglycidyl ether of bisphenol A (DGEBA)/graphene composites. *J Mater. Chem. A* **1**, 5081–5088 (2013).
25. Liang, J. J. *et al.* Electromagnetic interference shielding of graphene/epoxy composites. *Carbon* **47**, 922–925 (2009).
26. Ma, J. *et al.* Covalently bonded interfaces for polymer/graphene composites. *J. Mater. Chem. A* **1**, 4255–4264 (2013).
27. Monti, M. *et al.* Morphology and electrical properties of graphene-epoxy nanocomposites obtained by different solvent assisted processing methods. *Compos. Pt. A-Appl. Sci. Manuf.* **46**, 166–172 (2013).
28. Kovtyukhova, N. I. *et al.* Layer-by-layer assembly of ultrathin composite films from micron-sized graphite oxide sheets and polycations. *Chem. Mater.* **11**, 771–778 (1999).
29. Geng, J. & Jung, H. Porphyrin Functionalized Graphene Sheets in Aqueous Suspensions: From the Preparation of Graphene Sheets to Highly Conductive Graphene Films. *J. Phys. Chem. C* **114**, 8227–8234 (2010).

Acknowledgments

Author contributions

Y.L. conceived and designed the project. Y.L., Y.S., K.P. and S.A. fabricated the materials and carried the experiments. All authors contributed to the data and discussions regarding the research. Y.L. and K.L. wrote the manuscript.

Additional information

Supplementary information accompanies this paper at http://www.nature.com/scientificreports

Competing financial interests: The authors declare no competing financial interests.

How to cite this article: Li, Y., Samad, Y.A., Polychronopoulou, K., Alhassan, S.M. & Liao, K. Highly Electrically Conductive Nanocomposites Based on Polymer-Infused Graphene Sponges. *Sci. Rep.* **4**, 4652; DOI:10.1038/srep04652 (2014).